RESEARCH ARTICLE

Rate and Equilibrium Constants for Bupivacaine's Binding to Isolated Alpha-1-Acid Glycoprotein: An In vitro study.

Authors
Gary R. Strichartz[1] , Douglas E. Raines[2], Lawrence P. Cogswell III[1]

Affiliations
[1.] Pain Research Center, Department of Anesthesiology, Perioperative and Pain Medicine, Brigham and Women's Hospital and
[2.] Department of Anesthesia and Critical Care Medicine, Massachusetts General Hospital (DER), Harvard Medical School, Boston, MA 02115.

Corresponding author:
Dr. Strichartz at:
BWH/MRB611
75 Francis Street
Boston, MA 02115-6110
Ph: (617) 732-7802
Fx: (617) 730-2801
E-mail: gstrichartz@bwh.harvard.edu

Abstract
Binding of local anesthetics to plasma proteins has been presented as an important determinant of their bioavailability. Local anesthetics with a high potential for systemic toxicity, e.g. bupivacaine (BUP), are bound strongly by alpha$_1$-acid glycoprotein (AAG), more weakly by serum albumin, but drug dissociation may be rapid, thus limiting the importance of protein binding. The purpose of this study was to determine the binding kinetics of BUP to AAG. Bupivacaine binding to AAG was monitored by its displacement of the fluorescent probe 1-anilinonaphthalene-8-sulfonic acid (ANS). The increased fluorescence of ANS ($\lambda_{excit/em}$ = 380/480 nm) upon binding to AAG was used to determine the equilibrium and kinetic characteristics of this reaction. By studying how BUP altered the binding kinetics of ANS to AAG it was possible to calculate the BUPs equilibrium and kinetic rate constants for AAG binding. ANS fluorescence increased ca. 50-fold when bound to AAG. Increasing *[BUP]* with a constant *[AAG] + [ANS]* returned ANS fluorescence to its unbound status, due to complete displacement of ANS from AAG; bupivacaine's competitive equilibrium constant, K_i , equals 1-2 μM (pH 7.4, 23°C). Pre-equilibrating AAG with BUP before the rapid (0.008s) addition of excess ANS slowed the binding of ANS to a rate limited by BUP's dissociation: k_{off} = 12.0 ± 0.5 s^{-1}, corresponding to a half-time ~0.06 seconds. Therefore, although much of the total serum BUP at toxic levels (2-4 μg/mL) will be bound by plasma proteins, dissociation from the tightest binding protein shows that drug is rapidly freed during organ perfusion, allowing newly unbound drug to permeate into the perfused tissues. The very rapid dissociation of BUP from AAG means that *equilibrium binding* is a very poor index of bio-availability and systemic toxicity of that local anesthetic.

Key words: Local anesthetic, bupivacaine, alpha-1-acid glycoprotein, plasma proteins, systemic toxicity.

1. Introduction

Many local anesthetics (LA) in the circulation are highly bound to plasma proteins, i.e., alpha-1-acid glycoprotein (AAG) and serum albumin. [1-3] Although a large fraction of the total drug is protein-bound at equilibrium, this binding is reversible, so that the kinetics of dissociation may be as important as the equilibrium binding for determining the drug's bio-availability. Consider that the toxicity of the LA bupivacaine (BUP) after accidental intravenous delivery is critically dependent on transfer into the heart, [4,5] and the therapeutic, anti-hyperalgesic actions of lidocaine during intentional intravenous infusion depends on its uptake into the nervous system.[6] Those drug-binding proteins act as a buffer in regulating the free BUP concentration, [7-9] and this buffering effect, set by the binding capacity and affinity of the proteins, must be evaluated in adjusting the dosage of a drug and considering its toxicity.[1,10] However, the kinetics of such binding are also important for the blood:organ distribution in non-equilibrium circumstances, such as when drugs are being slowly extracted by the kidney or when they are rapidly delivered, intentionally or accidentally, as a bolus into the circulation.

Alpha$_1$-acid glycoprotein is the major plasma protein that binds local anesthetics.[8,9] Therefore, measurement of LA-AAG equilibrium and kinetic constants, especially for drugs like BUP which are relatively hydrophobic and potentially highly toxic, is very important for the complete consideration of LA pharmacokinetics.

Fluorescence is a very sensitive method for studying ligand:protein interactions .[11] Unfortunately, clinically used LAs are either non-fluorescent or weakly fluorescent, and unlike many other drugs, they do not quench the intrinsic fluorescence of AAG. To examine LA binding, therefore, other fluorescent probes have been used. We previously developed a synthetic LA containing 2 iodine atoms, diethyl-di-iodocaine (DEDIC), that quenched about 80% of the tryptophan-related fluorescence of AAG when it bound with very high affinity (K_D~ 50 nM).[12] However, due to DEDIC's correspondingly slow dissociation rate, it could not be used to determine the faster binding kinetics of the LA's that competitively displaced it from AAG, e.g., lidocaine, bupivacaine.[13] In the present study, we have used 1-anilinonaphthalene-8 sulfonic acid (ANS) as a probe to establish a method to measure the BUP dissociation rate constant from AAG. Although ANS has been used previously as a fluorescence probe to study the equilibrium binding of small molecule drugs to AAG,[14,15] we now present detailed kinetic information on ANS binding to AAG, and for the first time determine BUP's dissociation rate constant from that plasma protein.

2.Materials and Methods

2.1 Reagents

Bupivacaine hydrochloride and human AAG were obtained from Sigma-Aldrich Chemicals (St. Louis, MO). 1-anilinonaphthalene-8-sulfonic acid (ANS) was purchased from Molecular Probes (Eugene, Oregon).

2.2 Solutions

All experiments were conducted in a *standard aqueous medium* (SAM), which contained 150 mM NaCl in doubly deionized (18Mohm-cm), highly purified, pyrogen-free water (Water Systems 5601, Millipore Corp, Woburn, MA), buffered

with a combination of 3 Good buffers [16]: 2 mM CAPS [3-(cyclohexylamino)-propanesulfonic acid, pK_a = 10.4], 2 mM BICINE [N,N-bis(2-hydroxyethyl) glycine, pK_a = 8.35], and 2 mM MES [2-(N-morpholino)-ethanesulfonic acid, pK_a = 6.15] monohydrate (all were obtained from Calbiochem-Behring Corp, La Jolla, CA) in order to provide a constant buffering capacity over the experimental pH range. All drug stock solutions were adjusted to pH 7.4. Bupivacaine was freshly made prior to use as a stock solution (1.0 mM) at room temperature, and diluted to desired concentrations in SAM.

2.3 Steady-state fluorescence measurements

Steady-state fluorescence spectra and fluorescence readings in the ratio mode were obtained with an Aminco spectrofluorimeter (model SPF-500™ C, Aminco, Urbana, IL) (using 3g/L rhodamine B in ethylene glycol as reference) with a xenon lamp and direct temperature control of the cuvette. The bandwidths of 4 nm and 10 nm were set for excitation and emission monochromators, respectively. A square quartz cuvette with light pathlength of 10 mm was used when collecting steady-state fluorescence data, and a magnetic stir bar used to provide rapid mixing (~ 1 sec) for additions by hand. Between scans or changing conditions cuvettes were cleaned with doubly deionized (18Mohm-cm), highly purified water and isopropanol (HPLC grade, UV cutoff 205 nm, Fisher Scientific, Fair Lawn, NJ), and dried over air passed through a 0.2-μM filter (Gelman PTFE ACRO-disk).

2.4 Analysis of steady-state fluorescence data

To measure the K_D values for ANS binding to AAG, successive aliquots of ANS were added to a cuvette containing 2 mL of AAG solution, and the changes in ANS' fluorescence determined as a function of its final concentration, after several corrections, noted below. (To minimize photo-degradation during repeated excitation of the sample, single excitation and emission wavelengths were used (λ_{ex}=380 nm, λ_{em}=480 nm) and the excitation shutters were closed between readings.) Raw fluorescence data were first corrected for dilution effects and then normalized to unity, by dividing by the maximum fluorescence intensity, and plotted versus nominal concentrations of ANS. Analogous treatments were applied to bupivacaine competitive displacement experiments in which AAG and ANS concentrations were kept relatively constant and [BUP] was increased stepwise until no further decrease of ANS fluorescence occurred. The corrected and normalized fluorescence intensity were fitted by a one-site binding equation for extracting K_D value of ANS [12] or a one-site competition equation for extracting K_i values of drugs,[13] at equilibrium binding.

2.5 Kinetic measurements

Kinetic data were collected with an SX.18MV stopped-flow spectrofluorimeter (Applied Photophysics, Leatherhead, U.K.) with excitation at 380 nm. AAG (with or without ANS or BUP) solution was loaded into one of the spectrofluorometer's gastight mixing syringes, and ANS or BUP in SAM was loaded into the other. The two solutions were rapidly mixed at 1:1 volume ratio. The intensity of emitted fluorescence, after passing through a 503.2 nm cutoff filter with 15 nm half-width (Heliotek, Textron

Inc., Sylmar, CA), was recorded on a linear time base (1000 points over 0.5 s). For each experiment, five individual traces were averaged to improve the signal:noise ratio. All kinetic experiments were performed at 20.0 ± 0.2ºC. A double exponential equation (see below) was used to fit the curve to extract two amplitudes and their respective time constants that accounted for all the time-dependent signal. All reported concentrations in kinetic studies were post-mixing concentrations, unless otherwise indicated.

2.6 Statistical Analysis

Data here are reported as means ± SEM. Differences between binding constants, e.g. at two pH values, are compared by unpaired Student's t-test. $P<0.05$ was considered significantly different.

3.Results

3.1 ANS binds tightly to AAG.

ANS in solution is excited directly at wavelengths of 350-380 nm and emits maximally at ca. 530 nm, at pH 7.4, 23°C (Figure 1A, dotted line). When bound to AAG, ANS fluorescence properties are changed; its emission maximum is "blue-shifted" by 50 nm, to about 480 nm, and its fluorescence intensity is greatly increased (Figure 1A, solid line), consistent with its binding to a hydrophobic portion of the protein [17,18] Protein-bound ANS can be indirectly excited; by illuminating Trp residues in AAG at 280 nm, fluorescence energy is non-radiatively transferred to the bound ANS, which fluoresces 480nm. Such energy transfer-dependent signals occur only when the fluorescing ligands are within 10-20A of the excited Trp.[19] Indirectly excited ANS fluorescence reached its maximum when [ANS] was about stoichiometrically equal to all the AAG protein molecules (data not shown). These results show that ANS binds directly to AAG at the protein's hydrophobic regions, and does so with relatively high affinity.

We monitored the interactions between BUP and AAG by the reduction ANS' fluorescence due to its displacement from the protein. In all these experiments ANS was directly excited at 380 nm, and fluorescence measured at 480 nm, because BUP absorbs broadly around 240-290 nm, and would quench the excitation of Trp (280 nm). Figure 1A shows an example of AAG's reduced fluorescence when BUP is present with the local anesthetic and AAG (dashed line).

Figure 1B shows the directly excited fluorescence increase as an increasing amount of ANS is added to solutions containing three different AAG concentrations. The maximum fluorescence intensity at saturating ANS concentrations is proportional to the initial AAG concentration, and half saturation occurs at [ANS] below those of AAG, indicating a high affinity for the protein. When ligands bind with very high affinity, as happens here, such that saturation occurs at such low ligand concentrations that free [ligand] is substantially reduced from its initial value by its binding, then the apparent EC50 is far larger than the true K_D.[12] For example, half the maximum fluorescence from ANS binding to 1μM AAG occurs at a "nominal", starting [ANS] of ~0.7 μM, read from the x-axis of Figure 1B (solid circles), but if this situation corresponds to half occupancy of one site on each AAG molecule, then 0.5 μM ANS will be bound, leaving a true free concentration of 0.2μM. Equations that calculate the true K_D values in these situations were used to generate curves that simultaneously fit the experimental

data for all three AAG concentrations, giving an equilibrium dissociation constant (K_D) of ANS = 0.23 ± 0.15 μM (n=6) for binding to AAG at pH 7.4 and 23°C.

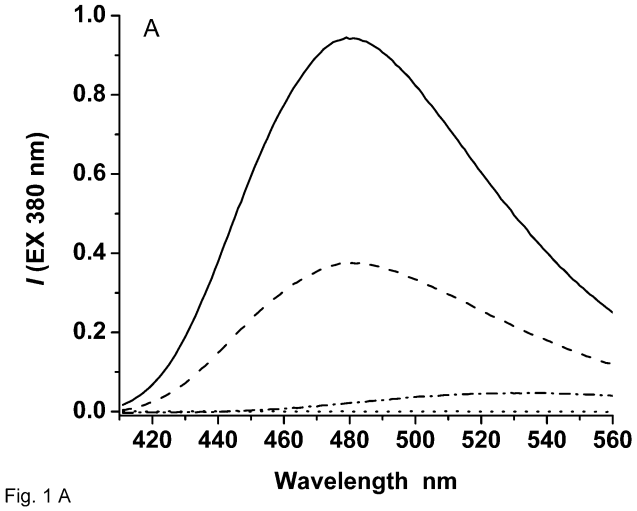

Fig. 1 A

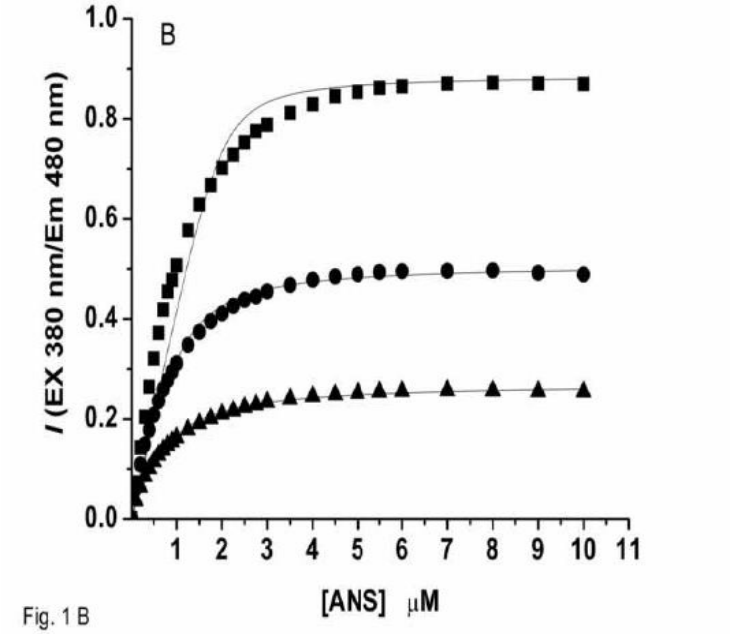

Fig. 1 B

Fig. 1. (A) Emission spectra of: 10 μM ANS alone (dash-dotted line); 1 μM AAG alone (dotted line); 1 μM AAG + 10 μM ANS (solid line); 1 μM AAG + 10 μM ANS + 20 μM BUP (dashed line), all at pH 7.4, 23°C. (B) Fluorescence monitoring of titration of ANS into 2.0 μM (■), 1.0 μM (●) and 0.5 μM (▲) AAG, at pH 7.4, 23°C. Data points are individual measurements from one experiment; the curves are derived from fits to data from 6 identical experiments, using equations for the one-site binding isotherm (ref. 12) to calculate the apparent *K*D of ANS = 0.23 ±0.15 μM (n=6).

3.2 Competitive equilibrium binding between ANS and BUP.

Bupivacaine competitively inhibited ANS binding to AAG. Titration of BUP into a pre-equilibrated AAG-ANS solution decreased ANS' fluorescence intensity, indicating the displacement of bound ANS by BUP (Figures 1A, 2). (In a reciprocal manner, titration of ANS into a pre-equilibrated BUP-AAG solution increased the fluorescence with a higher apparent K_D than without BUP, showing that ANS can competitively displace BUP from its binding site on AAG; data not shown.) There is almost zero residual fluorescence from ANS when BUP is taken to high concentrations, indicating that all bound ANS is displaced by BUP (Figure 2), Furthermore, the data in Figure 2 can be fit by a one-site binding competition model,[13] showing that only one BUP is required to displace one ANS from its binding site. The EC_{50} for this displacement reaction is 2.65±0.48 μM at 23 °C and pH 7.4, comparable to the K_D value of 2.97±0.23 μM for BUP binding to the F1*S variant [13] which species accounts for ~80% of the protein in whole AAG.[20]

Bupivacaine's affinity for AAG depends on pH. Raising the pH to 8.4, and thus increasing the fraction of BUP in the neutral base form ca. 5-fold, increased the LA's affinity approximately 3-fold, with a K_D value = 0.88±0.27 μM (n=3), significantly lower than the value at pH 7.4 ($p<0.05$, Student's t-test; Figure 2). This result shows that the neutral base binds more tightly than the charged cationic species, in agreement with earlier observations for BUP binding to whole AAG [8] and for lidocaine binding to the purified F1*S variant,[13] both measured using methods other than ANS displacement.

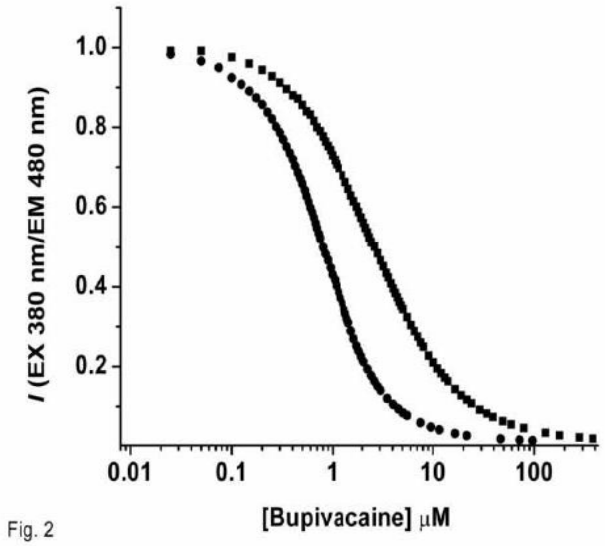

Fig. 2. Fluorescence enhancement from 2 μM ANS pre-equilibrated 2 μM AAG is reversed by increasing concentrations of bupivacaine; at pH 7.4 (■) and pH 8.4(●), both at 23° C. The data, averaged from three separate experiments, were fitted to a one-site competitive binding equation to calculate an apparent *K*i of BUP (see refs, 12,13). For pH 7.4, *K*i BUP = 2.65±0.48 μM (n=3) and for pH 8.4, *Ki* BUP= 0.885 ±0.27 μM (n=3).

3.3 ANS binds to AAG with multiple kinetic components.

When ANS is rapidly mixed with AAG, in a stopped-flow device mounted to a spectrofluorometer, the time-course of the fluorescence signal reflects the kinetics of ANS binding to the protein. In Figure 3, for example, the solid line from addition of 10 μM ANS to 1 μM AAG shows three components: one is too fast to be resolved within the ~1 msec mixing time of the instrument and is called the "immediate component", the second change is termed the "fast component" (4-20 ms) and the third the "slow component" (30-70 ms) of ANS binding. These two latter processes could be resolved by fits to the experimental data of a function with two exponential processes. Each of these processes, immediate, fast and slow, has a corresponding amplitude that depends on the concentration of ANS (Figure 4). The apparent EC_{50} for ANS equilibrium binding to 1 μM AAG, ca. 0.71 μM (Figure 1B), is the same as that for the summed amplitudes of the 3 transient components, ca 0.74 μM (Figure 4). However, total ΔF, from the sum of the transients analyzed kinetically, continues to rise with increasing [ANS] (Figure 4), which is different from the constant, saturating value of ΔF with increasing [ANS] measured in equilibrium experiments (Figure 1B). One explanation for this discrepancy is that the hypothetical *transient*, non-equilibrium states that occur early after ANS' initial binding result in higher fluorescence intensity than occurs when conformational changes have relaxed AAG to its equilibrium conformation (see Discussion).

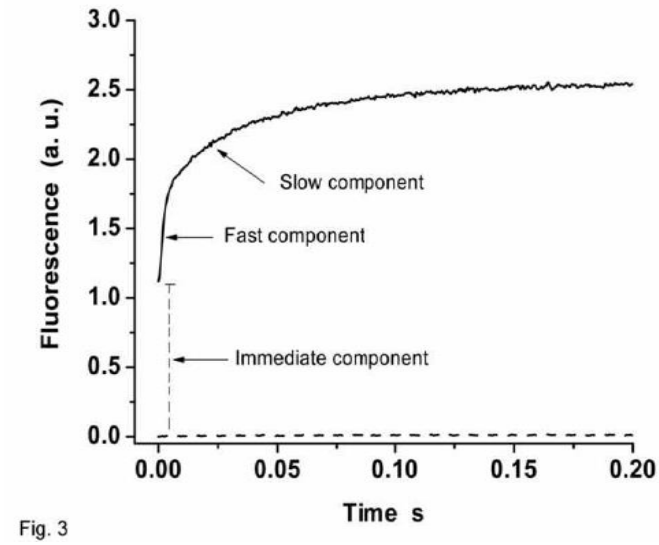

Fig. 3

Fig. 3. Typical time-course of fluorescence increase upon the binding of 10.0 μM ANS to 1.0 μM AAG (solid line) at 20°C, pH 7.4 The control experiment mixed the vehicle (SAM) instead of ANS (horizontal dashed line). The experimental curves were fitted with a sum of two exponentials to extract amplitudes and respective time constants (τ_f and τ_s) for "fast" and "slow" phases of the fluorescence increase.

The amplitude of the immediate component is almost proportional to [ANS], up to 10 μM, suggesting that this binding component is far from saturating at this concentration and corresponds to relatively low affinity binding (Figure 4).

In contrast, the fast component's amplitude rises steeply at low [ANS], peaking at 1-2 μM and then gradually decreasing as [ANS] increases further. This peak signal occurs near the concentration of AAG, 1 μM, and thus may arise from a saturation of high-affinity sites on the protein. A similar observation on ligand binding behavior was previously reported for halothane binding to a synthetic four-α-helix bundle protein.[21]

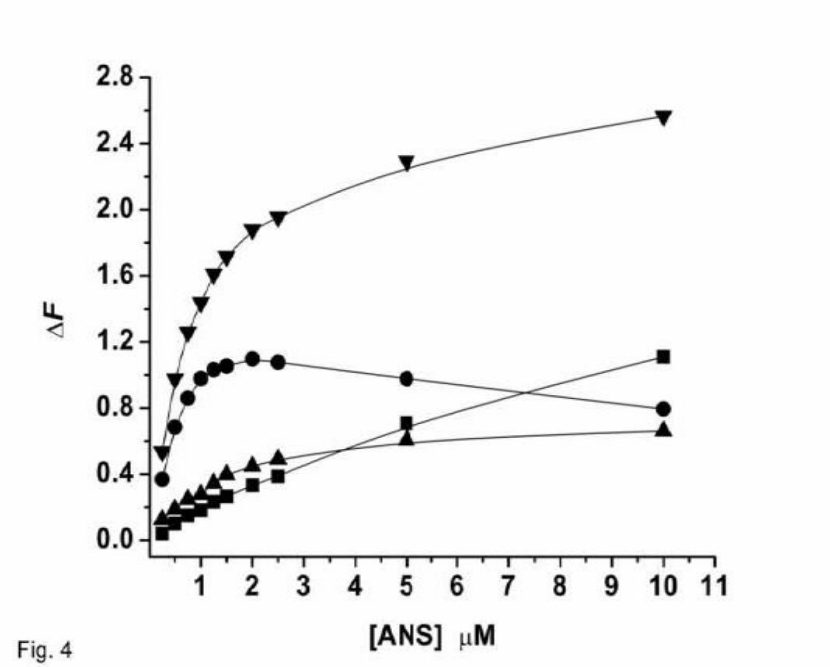

Fig. 4. The ANS concentration-dependence of the amplitudes of the "immediate" (■), "fast" (●), and "slow" (▲) phases of the fluorescence increases upon binding to AAG, and the total increase from the sum of these three extracted amplitudes (▼), at pH 7.4, 20°C.

The respective rates for the fast and slow processes, expressed as inverse time-constants derived from the exponential fitting, can also be compared for their ANS concentration-dependence (Figure 5). The rate (inverse time-constant) for the fast component increases approximately proportionately to [ANS], up to 5 μM (filled circles), behavior that describes a classic bi-molecular reaction:

$$\text{ANS} + \text{AAG} \underset{k_{off}}{\overset{k_{on}}{\rightleftharpoons}} \text{ANS-AAG} \qquad \text{(Eq. 1)}$$

The rate constants are related to the measured inverse time constant by:

$$\tau^{-1} = (k_{on}[\text{ANS}] + k_{off}) \qquad \text{(Eq. 2)}$$

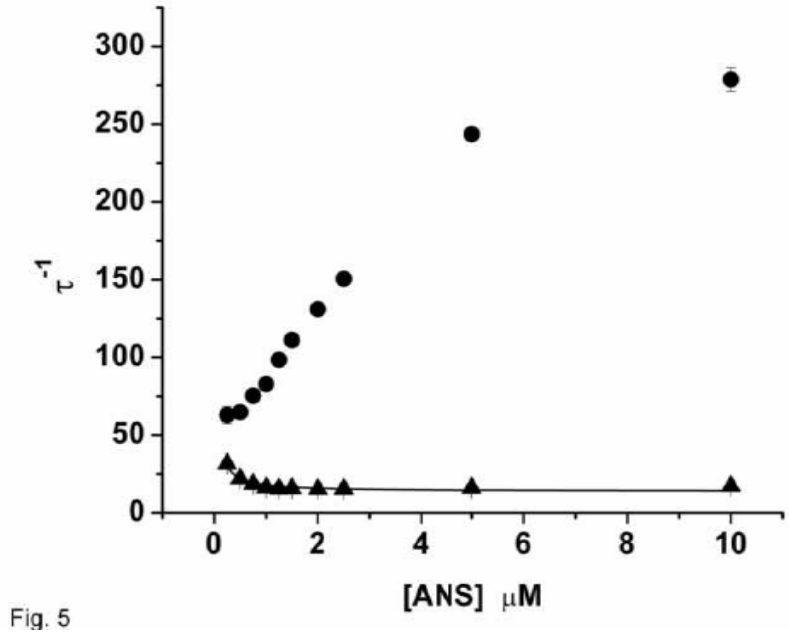

Fig. 5

Fig. 5. Graph of inverse time constants of the "fast" and "slow" components *versus* ANS concentrations. Rate constants $k1$ = 4.65 ±0.26 X 10^7 M^{-1} s^{-1} and k-1 = 41.6 ±1.8 s^{-1} were calculated from fitting of Equation 2 (see Results) to the inverse time constant for the fast component (●) over the range where it is proportional to [ANS] (up to 5 μM), with a correlation coefficient of 0.998. The slow component (▲) was fitted by Equation 3 to calculate k-2 = 3.48 X $10^6$$s^{-1}$, $k2$ = -3.48 X10^6 s^{-1} and K1 = 1.20x10^{-6}M. The negative $k2$ value is due to the fact that curve for the slow component is downward hyperbolic. An empirical third order polynomial function was used to fit the slow component's asymptote of 16.0±0.3 s^{-1}.

with k_{on} = 4.65 ± 0.26 × 10^7 M^{-1} s^{-1} and k_{off} = 41.6 ± 1.8 s^{-1} determined from fits of equation 2 to the data of Figure 5.

That the linear relation between the fast rate and [ANS] holds through 5μM and shows that the equilibrium amplitude maximum at 1-2μM (Figure 4) is not due to any kinetic restriction on the rate-limiting binding reaction.

The slow component's amplitude also increases almost linearly with [ANS], up to about 1.5 μM, then begins to show saturation but continues to grow continuously as [ANS] increases (Figure 4). Curiously, rates for the slow component actually decrease slightly over a low ANS concentration range, 0.25-1.5 μM, but then reach a relatively constant value of 16.0±0.3 s^{-1} (Figure 5), showing that the rates of this slow process become [ANS]-independent, even as the amplitude continues to increase. Since the slow, effectively zeroth-order, process has kinetics that are relatively independent of [ANS], it cannot be equated with a reaction of the protein directly with free ANS.

The dependence of the inverse time constant of the slow component on [ANS] was fitted by the equation:

$$\tau^{-1} = k_{-2} + k_2 K_1[\mathrm{ANS}]/(1+K_1[\mathrm{ANS}]) \qquad \text{(Eq. 3)}$$

which describes a rapidly equilibrating bi-molecular reaction, with equilibrium dissociation constant K_1, coupled to a slower, zeroth order process:[22]

$$\text{ANS} + \text{AAG} \underset{k_{-2}}{\overset{K_1}{\leftrightarrow}} \text{ANS·AAG} \overset{k_2}{\rightarrow} \text{ANS·AAG*} \quad \text{(Scheme 1)}$$

The best fit curve of equation 3 to these data has equal forward and reverse zeroth-order rate constants $k_{-2} = 3.48 \times 10^6\ s^{-1}$, $k_2 = -3.48\ s^{-1} \times 10^6$ and an equilibrium constant $K_1 = 1.20 \times 10^{-6}$ M (see Discussion). The negative k_2 value reflects the fact that the curve of τ^{-1} *vs* [ANS] for the slow component curves downwards. (Possible explanations for the apparent decrease in rate as [ANS] increases are presented in the Discussion, below.) The equilibrium constant for the fast component, $K_1 = 1.2 \times 10^{-6}$ M, is close to the value obtained by calculation of k_{-1}/k_1 (k_{off}/k_{on}) = 0.89×10^{-6} M using rates from the independently determined kinetics of the fast process (see above).

3.4 Bupivacaine's rapid dissociation from AAG.

Bupivacaine's dissociation rate constants were determined by experiments in which an excess of ANS was mixed with a pre-equilibrated solution of AAG and bupivacaine in which most of the protein was already bound by the local anesthetic. The AAG-bound BUP was replaced by ANS as the new equilibrium was reached, but because of their mutually excluding, competitive interaction, ANS could not bind until BUP had dissociated from the respective site on the protein. In other words, when the overall association rate of ANS (k_{ANS} X [ANS]) is much larger than the overall association rate of BUP (k_{BUP} X [BUP]), then virtually every molecule of BUP that dissociates from AAG will be replaced by a molecule of ANS. Also under these conditions, the dissociation rate of BUP becomes the *rate-limiting step* for ANS binding, as shown by the increase of fluorescence. A typical trace for ANS binding to AAG pre-equilibrated with BUP is shown by curve A in Figure 6, in which curve B is the reaction in the absence of BUP (copied from Figure 3). For AAG that has been pre-equilibrated with 5 μM BUP, the "immediate component" of ANS binding was greatly reduced. The remaining time-dependent changes of fluorescence were fitted, as above, with a double exponential function to extract time constants and amplitudes for the fast and slow components.

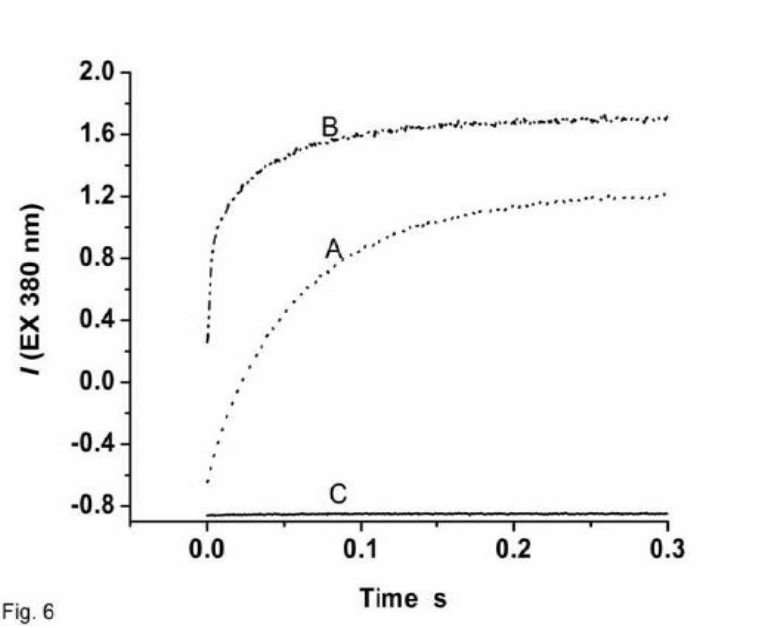

Fig. 6

Fig.6. Time course of the displacement of BUP (5 μM) bound to 1 μM AAG by 10μM ANS at 20°C, pH 7.4 (curve A). The result of adding 10 μM ANS to 1 μM AAG without any BUP (dotted line, curve B) and of adding an equal volume of buffer (SAM) to 1 μM AAG (solid line, curve C) are shown for comparison. The slower increase of fluorescence when AAG is pre-equilibrated with BUP reflects the rate-limiting dissociation of the local anesthetic in order for ANS to bind to the protein.

The final, steady-state fluorescence changes from ANS binding were reduced by pre-equilibrating AAG with BUP. (Since the ANS and BUP-AAG solutions are mixed in equal volumes to begin the reaction, the actual BUP concentration pre-equilibrated with AAG was twice that after mixing, the value listed on the x-axes of Figures 7 and 8). The kinetic parameters for "5 μM " BUP, for example, correspond to ANS (20 μM) binding to AAG (2 μM) which had equilibrated with 10 μM BUP, a concentration that occupies more than 95% of the ANS binding sites; see Figure 2). The amplitude of the "immediate" component is strongly reduced by this highest [BUP], by about 80%, consistent with a relatively low affinity for ANS in this site; the IC_{50} of BUP for this "immediate" inhibition, determined by finding the [BUP] on Figure 7 that gives half its maximum effect, is about 1μM. The "fast" component is reduced less, by only 30%, with an IC_{50} for BUP of <0.25μM. Unexpectedly, the amplitude of the "slow" component is actually increased, by ~2-fold; the apparent IC_{50} for this effect is also <0.25 μM, and the maximum increase in ΔF is reached at 0.5-1.0μM BUP (Figure 7).

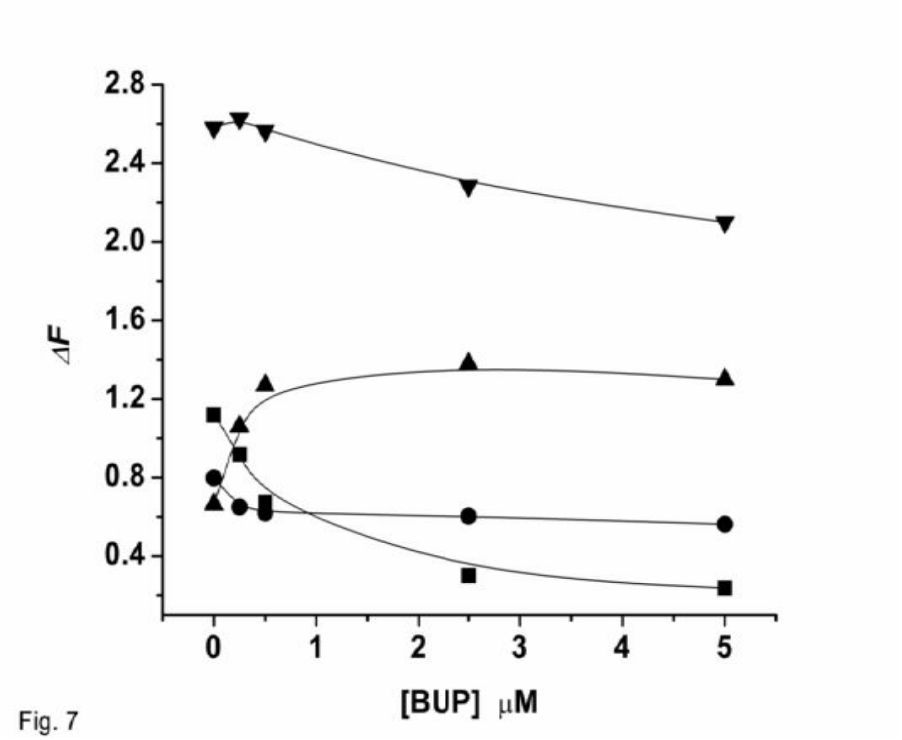

Fig. 7. The effect of increasing BUP concentration on the amplitudes of the immediate (■), fast (●), slow (▲) and total (▼) fluorescence changes upon mixing 10 μM ANS with 1 μM AGP pre-equilibrated with various concentration of BUP, at pH 7.4, 20°C.

Analysis of the kinetics of ANS-related fluorescence changes shows that BUP reduces the rates of both fast and slow components (Figure 8). As [BUP] increases, the fast component's rate drops by 88%, towards an asymptotic value of about 35 s^{-1} for 1μM ANS (not shown) and 39 s^{-1} for 10 μM ANS. These values are approximately equal to the k_{-1} for ANS dissociation derived from analysis of the fast process (see above). This agreement in rates is consistent with a competitive inhibition by BUP of the fast association step for ANS binding to AAG, and no effect of BUP on the fast dissociation step, requiring that the reduction in the fast amplitude is due completely to a reduction in the rate of binding of ANS to AAG. The slow component's rate, which was already lowered by this high [ANS] (Figure 5), is slightly reduced, by about 33%, and all within the same range of [BUP] that caused the increase in its amplitude (Figure 7). If, as described above, these rates reflect the dissociation of BUP from ANS binding sites on AAG, then the apparent rate-limiting dissociation rate of BUP is about 10- 30 s^{-1}.

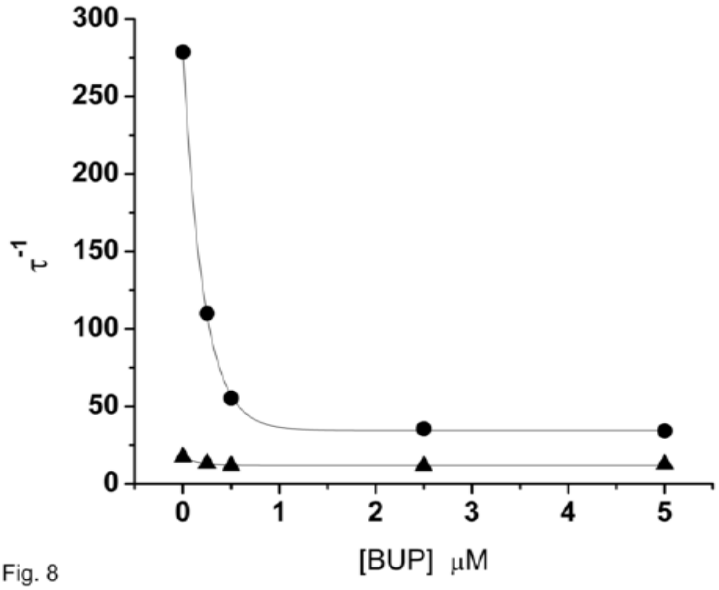

Fig. 8

Fig. 8. Graph of the inverse time constants of the fast (●) and slow (▲) components of the fluorescence changes from 10 μM ANS binding to AGP pre-equilibrated with different BUP concentrations; pH 7.4, 20°C. The data were fit by the empirical equation $\tau^{-1}=A*\exp(-B/[BUP])+\tau^{-1}{}_0$, to show the asymptotes ($\tau^{-1}{}_0$) of 34.5±1.1 s^{-1} (●) and 12.0±0.5 s^{-1} (▲) for the respective fast and slow components at saturating BUP concentrations (where A is τ^{-1} when [BUP] =0 and B is an empirical constant that fits the falling portion of the curves).

4. Discussion

4.1 Summary findings.

The findings of this investigation are: 1. ANS binds to AAG with 3 kinetic processes: one "immediate", kinetically unresolvable reaction, and two others, the "fast" one being a simple, first-order (bimolecular) reaction and the "slow" one a reaction independent of free ANS and possibly coupled to the faster binding step. 2. Bupivacaine can competitively antagonize all of the ANS binding at equilibrium, most potently for the "immediate" binding, less so for the "fast" binding", yet appears to enhance the amplitude of the "slow" binding process. Pre-equilibration of AAG with bupivacaine strongly reduces the rate of the fast reaction of ANS and reduces the slow reaction rate by far less. As an overall result, ANS binding rates at high [BUP] are limited by BUP's dissociation from AAG. These data show that the notion that LAs such as bupivacaine, when bound to AAG in the blood, are therefore unavailable to be resorbed from the circulation, is wrong.

4.2 Comparison with published observations.

Our observations agree with published equilibrium results in several respects. First, from the multiple components of its binding kinetics, it appears that there are at least two sites for ANS on AAG, and both of these sites are competed for by bupivacaine. Alpha-1 acid glycoprotein is member of the "lipocalin" group of proteins, soluble, carbohydrate-coupled molecules whose biological role is as carriers of small

molecules, odorants, cholesterol, etc.. [23] One common structural feature of all lipocalins is the presence of a "beta barrel" binding pocket where the ligands are proposed to bind, as verified by x-ray crystallography of many lipocalins, including AAG.[23,24] Tryptophan residues are located within the beta barrel as well as at more distant sites on the lipocalins.[17] We have previously reported the quenching of AAG's Trp-related fluorescence by the model local anesthetic, 2-hydroxy-3,5,-diiodo-N-[2(diethylamino)ethyl]benzamide (DEDIC), a functional local anesthetic containing 2 iodine atoms.[12] The concentration-dependence of DEDIC's quenching of intrinsic Trps revealed two sites on each molecule of this protein (of which the *F1*S* variant was bound by DEDIC with higher affinity than the *A* variant[12]). The quenching of AAG by DEDIC, at both low and high affinity sites, could also be fully reversed by BUP, as was the case for ANS in the present study, and the apparent equilibrium affinities are almost identical, 2.5-3μM [13]. Two bupivacaine binding sites on whole AAG have also been reported by Herve' et al.[20] and by Mazoit et al.[9] , using the equilibrium dialysis method; the latter authors also concluded on the basis of fits to Scatchard plots that some degree of positive cooperativity occurred in this binding.

Second, the binding of a related, BIS-ANS molecule to another lipocalin, apolipoprotein-D (apo-D) has similar kinetic characteristics. BIS-ANS contains two, nearly identical hydrophobic domains at the opposite ends of a molecule almost twice as large as ANS, and, using fluorescence assays like the one employed here, but without the rate-limiting step of mixing solutions (they used the temperature jump relaxation method), Patel et al.[17] found diffusion-limited binding rates consistent with a site for BIS-ANS on the protein's surface. We also find such fast rates for the "immediate" binding step, which is complete within the mixing time of ~ 1 msec at 10^{-6} M ANS, corresponding to an on-rate constant of ~10^9 M^{-1} s^{-1}. A slower rate of fluorescence increase, independent of [BIS-ANS], was detected for BIS-ANS binding to apo-D, which was attributed to the formation of protein-drug dimers as the free end of a BIS-ANS molecule bound superficially to one apo-D engaged a second apo-D at its superficial site.[17] The relatively large and very hydrophobic BIS-ANS appears to be unable to reach the binding site within the pocket of apo-D. We also observe slower rates for ANS binding to AAG, one of which is independent of [ANS], but we interpret this step differently, and have no evidence that "monovalent" ANS can conjugate two AAG molecules.

4.3 Limitations. There are two complications in the comparison of chemistries among these different systems; the first is that the human AAG that we used is a composite of several variants of this protein, and the second is that bupivacaine is a racemic mixture of equal R- and S- enantiomers. With regard to the first concern, our earlier work showed that the *F1* and *S* variants, which are almost identical in primary sequence, and together account for 80-85% of AAG in mixed human protein,[20,25] bind BUP with almost the same affinity as the A variant,[12] consistent with the near identical equilibrium affinities reported for lidocaine binding to these same variants.[20] With regard to the second concern, the different enantiomers of BUP bind to the *F1*S* variant of AAG with similar affinities: K_D (R-BUP) = 2.36±0.10 μM and K_D (S-BUP) = 1.42±0.08 μM from DEDIC displacement experiments on

purified *F1*S*[13], and 1.62 and 3.69 μM, respectively, from equilibrium dialysis using whole AAG [9] , although the latter values depend critically on the ratio of BUP:AAG. Nevertheless, these published affinities are near the IC_{50} value of 2.65±0.48μM reported here for the racemic mixture. Therefore, both our findings with ANS and its competition by bupivacaine are in general qualitative and quantitative agreement with published results.

4.4Kinetic models that account for the results.

The kinetics of ANS binding to AAG show that there are three binding components: immediate, fast and slow. We propose the following reaction scheme to explain the kinetic findings (Scheme 2): one fast and independent binding reaction for the "immediate" phase and two, coupled reactions for the fast (first-order) and slow phases.

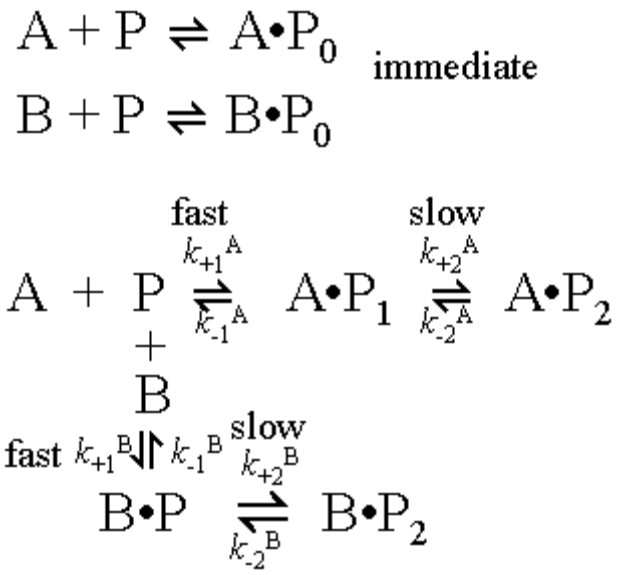

Scheme 2. Schematic presentation of competitive binding of AAG between ANS and BUP. A=ANS; B=BUP; P= AAG. P_0, P_1 and P_2 are conformations of AAG with different affinities for ANS and BUP.

This kinetic scheme accounts for the rate and equilibrium competitions between ANS and BUP. Consider first the [ANS] dependence of the different kinetic processes. The immediate component was too fast (within 1 ms) to have its kinetics resolved. Its amplitude is almost proportional to the nominal ANS concentration, up to 10 μM, and it is thus considered a low affinity site, probably at a superficial site on the protein. In contrast, the fast component has kinetics consistent with a bi-molecular reaction (up to about 5μM [ANS]), which we equate with the "fast" step in Scheme 2 (see Results and Figure 5).

The preceding analysis equates the added ANS that gives a "nominal concentration" with free ANS, but in situations where the high affinity of a ligand results in its binding at such low concentrations that the free concentrations is substantially less than the nominal one, the true affinity is always greater than the one calculated on the assumed equality between free and nominal ligand concentration. For example, the [ANS] to half-saturate the fluorescence change on binding to 1μM AAG is ca. 0.7 μM, but the

true K_D, when free [ANS] is corrected by accounting for the bound fraction, is ca. 0.25 μM (see Figure 1 and ref. 12). Accordingly, the actual concentrations of free ANS will change over the course of the binding reaction, dropping rapidly in the early times due to "immediate", albeit low affinity binding, and continuing to fall as the fast binding process progresses. This results in larger corrections for free [ANS] for the lowest nominal concentrations, becoming smaller as [ANS] increases. The net consequence is that the slope of the line for τ^{-1} *vs* [ANS] (Figure 5) will increase and so also will the calculated k_{+1}. Although an exact correction is impossible, since the immediate binding cannot be known, assuming that this fastest reaction is stoichiometric with AAG (at 1 μM) requires that the nominally assigned 2μM "free" ANS concentration be halved, approximately doubling the slope and the association rate constant. Further binding in the "fast" step will drop the free [ANS] even lower and effectively decrease the K_D, reaching that which is calculated from the precise equation that includes such binding[12], ca. 0.25 μM (Figure 1B).

The "fast" processes' amplitude shows a biphasic dependence on [ANS], peaking at 1-2μM. The slow component's amplitude also increases almost linearly with [ANS], up to about 1.5μM, then increases less steeply but still continuously as [ANS] increases (Figure 4). Scheme 2 provides an explanation for these observations, identifying the fast phase with a rapid binding reaction, which is coupled to a slower reaction that requires no additional binding. For relatively low [ANS] the fast binding results in only partial occupancy to form the species identified as AP_1, where little of the slow reaction occurs since k_{-1} is larger than k_{+2}. As the added [ANS] increases, however, and the increasing occupancy of AP_1 becomes a substantial source for AP_2 , the fast reaction will eventually slow and the amplitude of the fast component will be decreased.

There are two possible mechanistic explanations for the slow reaction. One is that the locus on AAG of a bound ANS molecule changes, allowing additional binding at P_1 when the initially bound ligand migrates to P_2. The other is that there is an ANS-induced conformational change [26] such that either the local milieu around the ANS molecule becomes more polar, thus reducing its quantum efficiency and lowering the fluorescence of bound ANS, or that a slow structural change of AAG after ANS binding changes the binding properties such that , for example, k_{-1} is increased and the affinity is thereby decreased.[27] In fact, both phenomena could occur, for if the binding domain becomes more polar, e.g., by movement of a charged amino acid, then either electrostatic or hydrophobic binding energy could be reduced, lowering both ANS affinity and quantum yield from the same change in the protein. These phenomena could also explain the cooperativity for bupivacaine binding observed by Mazoit et al.[9]

5. Conclusion

Our finding that there are multiple binding sites on AAG for BUP is novel, and may apply to other basic, amphipathic drugs, such as class I anti-arrhythmics and many anti-epileptics, that also are bound by AAG. AAG binding of BUP is of relatively high affinity and rapidly reversible; at the plasma concentrations where toxicity occurs, 2-4 μg/mL, equivalent to 7-15 μM, and AAG is at a high molar excess over BUP, 0.6-1.2mg/mL= 1.4-2.8mM. Of course, BUP binds to other serum proteins, e.g.

albumin, with a higher binding capacity although lower affinity,[28] and is adsorbed by the membranes of red and white cells in the blood, all of which reduce its free concentration and its potential to saturate the high affinity AAG binding sites.[2-4] Importantly, BUP's dissociation from AAG is quite rapid, despite its sub-micomolar equilibrium dissociation constant. The off rates of 10 s^{-1} mean that in 0.1 seconds more than half of AAG-bound bupivacaine would be liberated if the free plasma concentration suddenly fell to zero. Consequently, AAG-bound bupivacaine becomes quickly available for permeation through the capillaries, contributing to toxicity and metabolism as the drug-equilibrated plasma perfuses organs. The weaker binding of BUP to serum albumin will likely correspond to an even faster dissociation. We conclude that the application of equilibrium data for protein binding of local anesthetics to any pharmacokinetic understanding is virtually useless and potentially misleading.

Acknowledgment

Supported by grants from the USPHS, NIH: GM64792 (GRS) and GM58448 (DER). Most of the experiments and analyses reported here were conducted by Dr. Jingzhong Zhang, who was supported in part by a stipend from the BWH Foundation for Research and Teaching in Anesthesia. Regretfully, the authors have been unable to contact Dr. Zhang, who would otherwise, without question, be first author on this paper. The authors thank Ms. Ellen Jacobson for secretarial services.

References

1. Wood M and Wood AJ: Changes in plasma drug binding and alpha 1-acid glycoprotein in mother and newborn infant. *Clin Pharmacol Ther* 1981; 29:522-526
2. Routledge PA: The plasma protein binding of basic drugs." *Br J Clin Pharmacol* 1986; 22:499-506
3. Kremer JM, Wilting J and Janssen LH: Drug binding to human alpa-1-acid glycoprotein in health and disease. *Pharmacol Rev* 1988; 40:1-47
4. Kytta J, Heavner JE, Badgwell JM and Rosenberg PH: Cardiovascular and central nervous system effects of co-administered lidocaine and bupivacaine in piglets. *Reg Anesth* 1991; 16:89-94
5. Mazoit JX, Orhant EE, Boico O, Kantelip JP, Samii K: Myocardial uptake of bupivacaine: I. Pharmacokinetics and pharmacodynamics of lidocaine and bupivacaine in the isolated perfused rabbit heart. *Anesth Analg* 1993; 77:469-76
6. Chaplan SR, Bach FW, Shafer SL, Yaksh : Prolonged alleviation of tactile allodynia by intravenous lidocaine in neuropathic rats. *Anesthesiology* 1995; 83:775-85
7. Dauphin A, Gupta RN, Young YEM and Morton WD: Serum bupivacaine concentrations during continuous extrapleural infusion. *Can J Anaesth* 1997; 44:367-370
8. Denson D, Coyle D, Thompson G and Myers J. Alpha 1-acid glycoprotein and albumin in human serum bupivacaine binding. *Clin Pharmacol Ther* 1984; 35:409-415
9. Mazoit JX, Cao LS, Samii K: Binding of bupivacaine to human serum proteins, isolated albumin and isolated alpha-1-acid glycoprotein. Differences between the two enantiomers are partly due to cooperativity. *J Pharm Exp Ther* 1996; 276:109-115
10. Covino BG, Wildsmith JAW. Clinical pharmacology of local anesthetic agents, Neural Blockade in Clinical Anesthesia and Management of Pain, 3rd edition. Edited by Cousins MJ, Bridenbaugh PO. Philadelphia, *Lippincott-Raven*, 1998, pp.105-115
11. Parikh HH, McElwain K, Balasubramanian V, Leung W., Wong D, Morris ME and Ramanathan M. A rapid spectrofluorimetric technique for determining drug-serum protein binding suitable for high-throughput screening. *Pharm Res* 2000; 17:632-637
12. Cogswell LP, Raines DE, Parekh S, Jonas O, Maggio JE, Strichartz GR. Development of a novel probe for measuring drug binding to the F1*S variant of human alpha 1-acid glycoprotein. *J Pharm Sci* 2001; 90:1407-1423
13. Taheri S, Cogswell LP, Gent A and Strichartz GR: Hydrophobic and ionic factors in the binding of local anesthetics to the major variant of human alpha 1-acid glycoprotein. J *Pharmacol Exp Ther* 2003; 304:71-80
14. Zini R, Copigneaux C and Tillement JP: 1-anilino-naphthalene 8-sulfonic acid (ANS) as a probe for the binding of antidepressant drugs to human alpha-1-acid glycoprotein (AAG). *Prog Clin Biol Res* 1989; 300:417-421
15. Johansen AK, Willassen NP and Sager G. Fluorescence studies of beta-adrenergic ligand binding to alpha 1-acid glycoprotein with 1-anillio-8-naphthalene sulfonate, isoprenaline, adrenaline and propranolol. *Biochem Pharmacol* 1992; 43:725-729
16. Good NE, Winget GD, Winter W, Connolly TN, Izawa S and Singh RM: Hydrogen ion buffers for biological research. *Biochemistry* 1966; 5:467-477
17. Patel RC, Lange D, McConathy WJ, Patel YC and Patel SC: Probing the

structure of the ligand binding cavity of lipocalins by fluorescence spectroscopy. *Protein Eng* 1997; 10:621-625

18. Lackowicz JR: Fluorescence spectroscopy of biomolecules, Encyclopedia of Molecular Biology and Molecular Medicine. Edited by Meyers A. New York, *VCH Publishers*, 1995, pp294-306

19. Stryer L: Fluorescence energy transfer as a spectroscopic ruler. *Ann Rev Biochem* 2978; 47:819-846

20. Herve F, Duche JC, d'Athis P, Marche C, Barre J and Tillement JP: Binding of disopyramide, methadone, dipyridamole, chlorpromazine, lignocaine and progesterone to the two main genetic variants of human alpha 1-acid glycoprotein: evidence for drug binding differences between the variants and for the presence of two separate drug-binding sites on alpha 1-acid glycoprotein. *Pharmacogenetics* 1996; 6:403-415

21. Solt K, Johansson JS and Raines DE: "Kinetics of anesthetic-induced conformational transitions in a four-alpha-helix bundle protein." *Biochemistry* 2006; 45:1435-1441

22. Barbier P, Peyrot V, Dumortier C, D'Hoore A, Rener GA and Engelboroghs Y: Kinetics of association and dissociation of two enantiomers, NSC 613863 (4)- (+) and NSC 618862 (S)-(-) CL980, to tubulin. *Biochemistry* 1996; 35:2008-2015

23. Flower DR: The lipocalin protein family: structure and function. *Biochem J* 1996; 318:1-14

24. Schönfeld DL, Ravelli R, Mueller U, Skerra A. The 1.8-A crystal structure of alpha1-acid glycoprotein (Orosomucoid) solved by UV RIP reveals the broad drug-binding activity of this human plasma lipocalin. *J Mol Biol*. 2008;384(2):393-405. doi: 10.1016/j.jmb.2008.09.020. Epub 2008 Sep 16.

25. Herve F, d'Athis P, Tremblay D, Tillement JP and Barre J. Glycosylation study of the major genetic variants of human alpha 1-acid glycoprotein and of their pharmacokinetics in the rat. *J Chromatography B Analyt Technol Biomed Life Sci* 2003; 798:283-294

26. Pidikiti R, Zhang T, Mallela KM, Shamim M, Reddy KS and Johansson JS: Sevoflurane-induced structural change in a four-alpha-helix bundle protein. *Biochemistry* 2005; 44:12128-12135

27. Peters T. *All About Albumin: Biochemistry, Genetics and Medical Applications*. San Diego, CA: Academic Press Limited. 1996.

